THE 2002 RELEASE OF WAVEWATCH III [1]

Hendrik L. Tolman[2]

SAIC/GSO at NOAA/NCEP/EMC
Marine Modeling and Analysis Branch
5200 Auth Road Room 209, Camp Springs, MD 21746

1 INTRODUCTION

Since the early 1990s, the Marine Modeling and Analysis Branch (MMAB) of the Environmental Modeling Center (EMC) of the National Centers for Environmental Prediction (NCEP) has been developing the WAVEWATCH III ocean wave model. At NCEP, the combination of this generic wave model with wind products from NCEP is called NOAA WAVEWATCH III, or NWW3. NWW3 was accepted for operation use in 1998, and replaced all previous operational NOAA/NCEP wave models in March 2000 (see Tolman et al., 2002). The NWW3 model became officially operational at NCEP in March 2000, with a global model at $1.25°\times1.00°$ longitude-latitude resolution, and regional Alaskan Waters (AKW, $0.50°\times0.25°$) and Western North Atlantic (WNA, $0.25°\times0.25°$) models (see Tolman et al., 2002). In June 2001, the North Atlantic Hurricane wave model was added (NAH, see Chao and Tolman, 2001), using the same grid as the WNA model. In April 2002, the Eastern North Pacific model (ENP, $0.25°\times0.25°$), was added. A hurricane version of this model is planned for 2003.

The operational wave models at NCEP originally used version 1.18 of WAVEWATCH III (Tolman, 1999). The physics parameterizations in these models are based on Hasselmann et al. (1985), Tolman and Chalikov (1996) and Hasselmann et al. (1973). The numerical approaches are based on Leonard (1979, 1991) and Tolman (1992). Version 1.18 of WAVEWATCH III was publicly released in April 1999. Since then, more than 550 copies of the code have been requested worldwide through its web site[3]. Since 1999, significant development of the model has been undertaken. A new version of the model (version 2.22, Tolman, 2002d) has replaced version 1.18 in NCEP's operational models on August 13, 2002 . This model version has been made available to the community in September 2002. The present paper documents changes between the two model versions, and presents an outlook to the future. Version 1.18 will simply be denoted as the old model, and version 2.22 as the new model. A more elaborate documentation of the effects of all changes can be found in Tolman (2002b)

In section 2, core changes to the model are discussed, consisting of a transition to FORTRAN 90, and some minor changes to the integration scheme for the physics. In section 3 alternative methods to deal with the Garden Sprinkler Effect (GSE) are discussed. In section 4 a sub-grid representation of unresolved islands and ice is discussed, which triggered a need to revisit model tuning (section 5). Two additions to the code are not discussed here. They are the option to run the model on a Cartesian instead of spherical grid, and the option to include exact nonlinear interactions according to the Webb-Resio-Tracy method (Webb, 1978; Tracy and Resio, 1982; Resio and Perrie, 1991), curtesy of Van Vledder (2002). Both of these additions are made only for research purposes. Finally, a brief outlook to the future will be given in section 6.

[1] MMAB contribution Nr. 220
[2] E-mail:Hendrik.Tolman@NOAA.gov
[3] http://polar.ncep.noaa.gov/waves/wavewatch

2 CORE MODEL CHANGES

WAVEWATCH III was originally coded in ANSI standard FORTRAN 77, to maximize portability of the code. Since then, FORTRAN 90 has come to maturity, with reliable compilers available for virtually every platform. The entire wave model code has been converted to FORTRAN 90 for two main reasons. First, all relevant data structures have been made dynamically allocatable. This removes the need to pre-set array sizes in the model. Secondly, the code has been organized in modules, removing the need for COMMON data structures. These changes were made to simplify code maintenance and future code development. Along the way some minor changes in the order of calculations have been made. For all practical purposes, the move to FORTRAN 90 has no impact on model results (see Tolman, 2002b, section 2), but makes the code typically 5 to 10% slower (due to the dynamic allocation of memory).

Another change to the core of the wave model was made in the integration of the source terms. The source term step of the model solves the equation

$$\frac{\partial N(k,\theta)}{\partial t} = S(k,\theta) \quad , \tag{1}$$

where N is the spectrum, S represents the net source terms, and k and θ are the wavenumber and direction spanning spectral space. A semi-implicit integration scheme is used, with dynamically adjusted time step (WAMDIG, 1988; Tolman, 1992), where the discrete change of action density ΔN is calculated as

$$\Delta N(k,\theta) = \frac{S(k,\theta)}{1 - \epsilon D(k,\theta)\Delta t} \, , \tag{2}$$

where D represents the diagonal terms of the derivative of S with respect to N, The parameter ϵ defines the offset of the scheme. Originally, $\epsilon = 0.5$ was implemented to obtain a second order accurate scheme. Recent work by Hargreaves and Annan (1998, 2001) has shown that a forward in time scheme with $\epsilon = 1$ is more appropriate for the wave model. This approach is therefore adopted in the new model. In the new model, default setting of all parameters in the integration and physics schemes have been defined. The numerical parameters are set to make the schemes slightly more responsive to wind changes. These two changes to the integration schemes have been made to generate slightly smoother spectra at slightly reduced computational costs, but have little impact on bulk wave heights (see Tolman, 2002b, section 3).

3 GARDEN SPRINKLER EFFECT

Spatial wave propagation in wave models with discretized spectra is subject to the so-called Garden Sprinkler Effect (GSE, see Booij and Holthuijsen, 1987). If the spectral discretization is coarse, a continuously dispersing swell field will spuriously disintegrate into a small number of discrete swell fields, each propagating in discrete directions and with discrete speeds as determined by discrete spectral bins (k_i, θ_j). To alleviate this problem, the old model uses the modified discrete spatial propagation equations of Booij and Holthuijsen (1987) (note that refraction is treated separately)

$$\frac{\partial N}{\partial t} + \frac{\partial}{\partial x}\left[c_x N - D_{xx}\frac{\partial N}{\partial x}\right] + \frac{\partial}{\partial y}\left[c_y N - D_{yy}\frac{\partial N}{\partial y}\right] - 2D_{xy}\frac{\partial^2 N}{\partial x \partial y} = 0 \, , \tag{3}$$

where c_x and c_y are the advection velocity in the two spaces, and D_{xx}, D_{yy} and D_{xy} are the components of the diffusion tensor with main axis θ. This diffusion tensor is added to the conventional advection equation, to account for (spectral) sub-grid dispersion. This GSE alleviation method has been used successfully in the old model, but dramatically increases model run times for higher resolution regional models (Tolman, 2001, 2002a) due to more stringent stability criteria for the added diffusion terms in (3). For this reason, two alternative GSE alleviation methods have been developed, and are made available in the new model (for detailed descriptions, see Tolman, 2002a).

The first method replaces the diffusion tensor in Eq. (3) with a separate spatial averaging step, where the shape of the averaging area is determined by the mean direction for the spectral bin considered, and by the

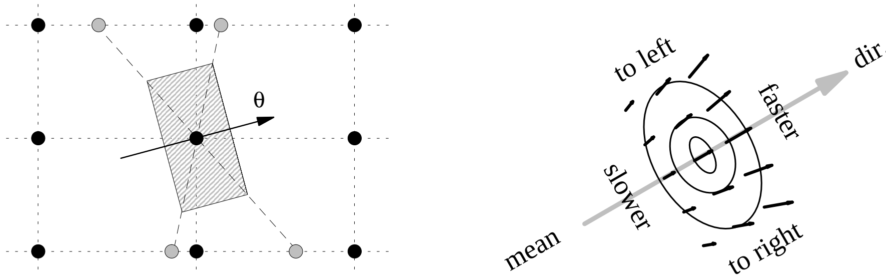

Fig. 1: Illustrations of alternative GSE alleviation methods from the new model (from Tolman, 2002d). Left: averaging technique. • and dashed lines represent grid points and lines. Shaded area represents averaging area. Right: divergent advection method, with systematic changes in advection speed and direction for discrete component of wave field.

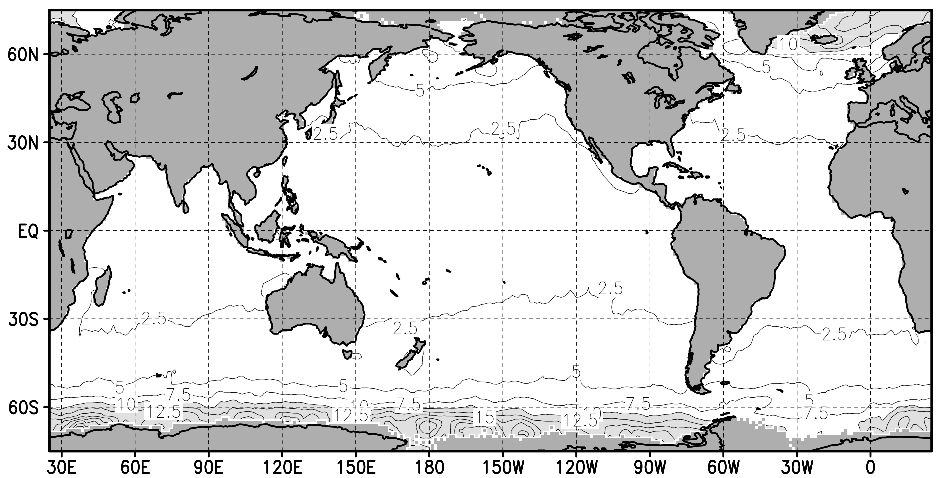

Fig. 2: March 2000 through February 2001 rms wave height differences along ERS-2 track in cm between old and new wave models due to change from Booij and Holthuijsen (1987) GSE alleviation technique to the Tolman (2002a) averaging technique. Light grey identifies rms > 10 cm.

spectral discretization. This averaging is closely related to the diffusion approach, but does not impact model time steps negatively. The results of this method are virtually identical to those of the Booij and Holthuijsen (1987) method, as is illustrated in Tolman (2002a,b), and in Fig. 2 with the rms differences between the old and new models for a one year hindcast with the global NWW3 model as described in Tolman (2002b). For most of the globe, the rms wave height differences between the models are much less than 10 cm. Only for high latitudes (past 60°N and S), more notable differences are found. For such latitudes, the old method needs to be suppressed for reasons of economy and/or stability, whereas the new method can still be used in full. Additional test results are presented in section 4 of Tolman (2002b).

The second method adds divergence to the advection velocity vector for a given spectral bin (right panel in Fig. 1), thus dispersing the energy in a given bin more realistically. This method proved very capable of removing the GSE, but turned out to be more expensive (Tolman, 2002a). For this reason the averaging technique is now designated as the default GSE alleviation method in WAVEWATCH III. For the tests as performed in Tolman (2002a), this method reduced the computational effort for large scale models by about 5%. The impact for the high-resolution NAH model was more impressive, with a reduction of computational costs of nearly 40%.

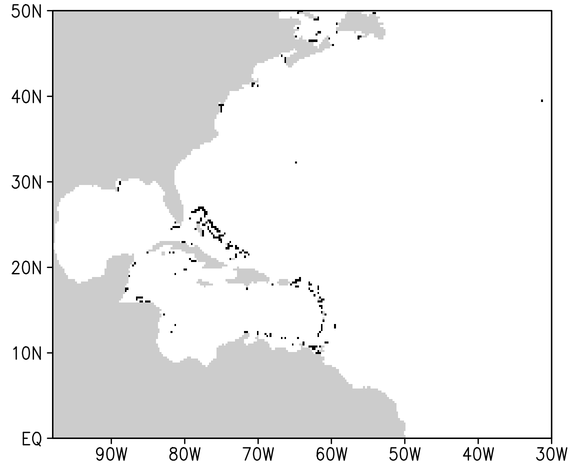

Fig. 3: Grid layout of the regional WNA wave model. Grey identifies land points, black identifies grid points with some obstruction in longitudinal or latitudinal direction ($\alpha \neq 1$). Note that this obstruction can be as small as 5%.

4 UNRESOLVED ISLANDS AND ICE

A major source of (local) errors in the old model are unresolved islands, where swell energy is dissipated in nature, but is left unchanged in the model (see Tolman, 2001; Tolman et al., 2002). In the new model, a sub-grid representation of unresolved islands is introduced, based on a similar approach from the SWAN model (Holthuijsen et al., 2001). For wave propagation in the x direction, the numerical schemes in WAVEWATCH III can be expressed as

$$N_l^{n+1} = N_i^n + \frac{\Delta t}{\Delta x}\left[\mathcal{N}_{l,-} - \mathcal{N}_{l,+}\right] \quad , \tag{4}$$

where l and n are discrete space and time counters, respectively, and where $\mathcal{N}_{l,-}$ is the discrete flux at the cell boundary between the grid points with counters l and $l-1$, and $\mathcal{N}_{l,+} = \mathcal{N}_{l+1,-}$. Sub-grid obstacles at cell boundaries can be included in Eq. (4) by changing this equation to

$$N_i^{n+1} = N_l^n + \frac{\Delta t}{\Delta x}\left[\alpha_{l,-}\mathcal{N}_{l,-} - \alpha_{l,+}\mathcal{N}_{l,+}\right] \quad , \tag{5}$$

where $\alpha_{l,-}$ and $\alpha_{l,+}$ are 'transparencies' of the corresponding cell boundaries, ranging from 0 (closed boundary) to 1 (no obstructions), and leaving outflow boundaries to be always fully transparent ($\alpha = 1$). Details of the incorporation of obstructions can be found in Tolman (2002c,d).

The introduction of sub-grid scale obstacles to represent islands, also opens the possibility of continuous treatment of ice coverage. Presently, ice coverage is used in wave models in a discontinuous way, removing grid points from the calculations (i.e., treating such grid points as land) if a critical ice concentration ϵ_c is reached, and ignoring ice otherwise. Following Tolman (2002c), a continuous ice model can be defined where wave propagation is not impeded for ice concentrations less than $\epsilon_{c,0}$, and is completely impeded for concentrations greater than $\epsilon_{c,n}$. From these concentrations, decay length scales l_0 and l_n are calculated as

$$l_0 = \epsilon_{c,0}\min(\Delta x, \Delta y) \quad , \quad l_n = \epsilon_{c,n}\min(\Delta x, \Delta y) \quad , \tag{6}$$

from which ice related transparencies are calculated as

$$\alpha_x = \begin{cases} 1 & \text{for} \quad \epsilon\Delta x < l_0 \\ 0 & \text{for} \quad \epsilon\Delta x > l_n \\ \frac{l_n - \epsilon\Delta x}{l_n - l_0} & \text{otherwise} \end{cases} \quad , \quad \alpha_y = \begin{cases} 1 & \text{for} \quad \epsilon\Delta y < l_0 \\ 0 & \text{for} \quad \epsilon\Delta y > l_n \\ \frac{l_n - \epsilon\Delta y}{l_n - l_0} & \text{otherwise} \end{cases} \quad . \tag{7}$$

The island and ice obstructions can than be combined by simple multiplication. A detailed discussion of these obstruction models as well as several extensive hindcast tests with NCEP's operational models are presented in section 5 of Tolman (2002b) and in Tolman (2002c). Some selected examples are given here.

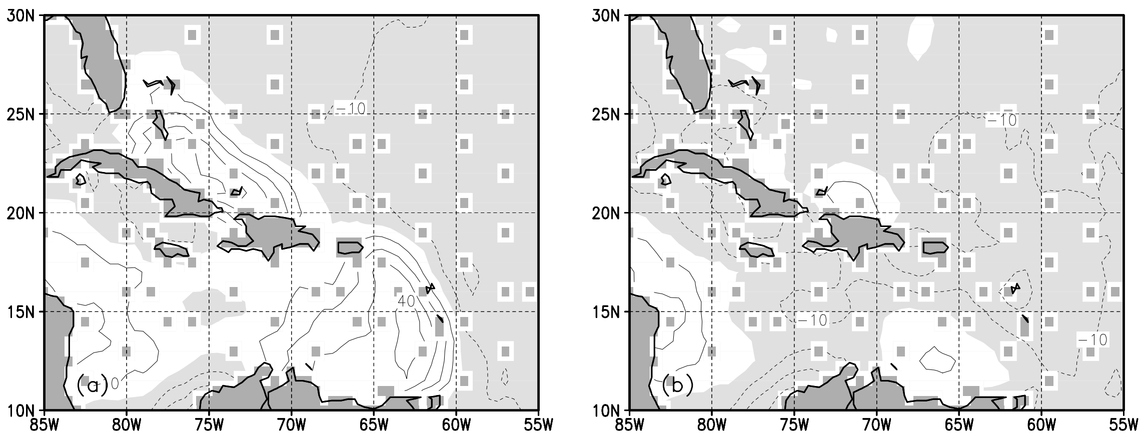

Fig. 4: Wave height biases in cm of the old and new WNA models against ERS-2 altimeter data for March 2000 through February 2001. Negative biases shaded light grey, contours at 10 cm intervals.

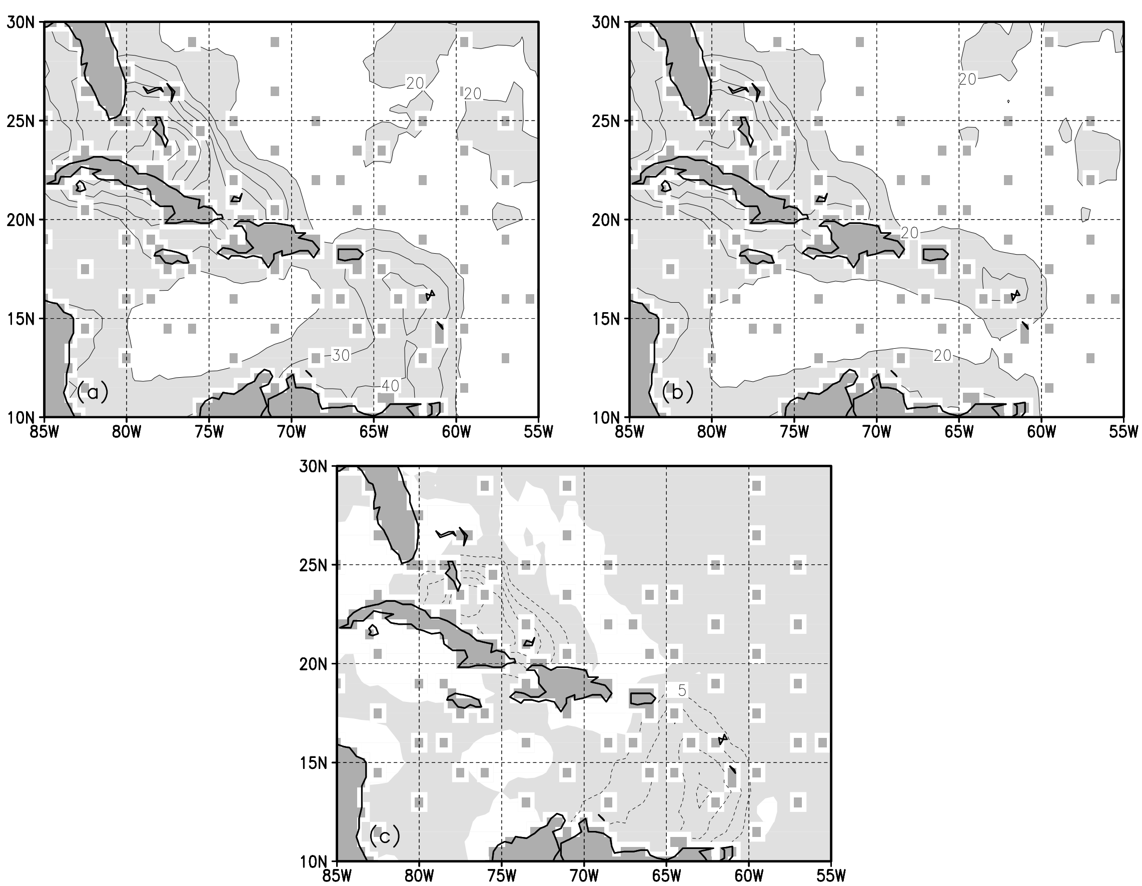

Fig. 5: Scatter indices (SI) in % (rms error normalized with mean observation) corresponding to Fig. 4. (a,b) old and new model, respectively, contours 10% intervals. Light grey shading for SI > 20%. (c) differences, contours at 5% interval, light grey shading identifies negative difference (model improvement)

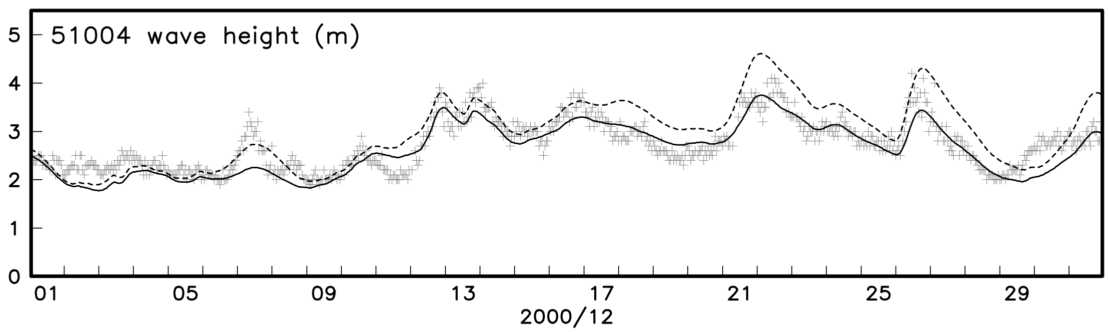

Fig. 6: Time series of wave height H_s observed at buoys (+), from the old global NWW3 model (dashed line) and from the new model (solid line) for buoy 51004 south of Hawaii for December 2000.

The effects of the sub-grid scale island representation will be discussed using the one year hindcast results for the regional WNA model. Even for such a relatively high resolution regional model, many important island groups are not properly resolved, as is illustrated in Fig. 3. Particularly, the Bahamas and the Lesser Antilles are not resolved by the grid. The effect of a sub-grid scale representation of islands is mostly restricted to areas near these islands. This is illustrated in Fig. 4 with wave height biases of the old and new model for a one year hindcast for the area of the WNA model covering the major unresolved island groups, based on ERS-2 altimeter data. The old model (Fig. 4a) shows clear positive biases of up to 0.50 m around the unresolved islands. In the new model (Fig. 4b) these positive biases are completely eliminated.

Figure 5 shows Scatter Indices (SI) of the old and new models, defined as the overall rms wave height error normalized with the mean observed wave height, based on ERS-2 observations. In the old model (Fig. 5a), Scatter Indices of over 40% are found near the Bahamas and the Lesser Antilles. In the new model (Fig. 5b), these errors are significantly reduced. This is particularly obvious in the differences in SI between the models (Fig. 5c). In the Lesser Antilles the SI is reduced by more than 20%, from more than 40% in the old model to less than 20% in the new model. Note that the remaining large SIs behind the Bahamas in the new model are partially due to the extremely small mean wave height used in the normalization here. In such conditions, the SI is a less representative error measure for a model.

Buoy locations in many cases are chosen to avoid areas obstructed by islands. Therefore, the effects of the sub-grid island representation are generally not obvious in collocations of model results and buoy data. Nevertheless, some exceptions occur. An example is given in Fig. 6 with results for the Hawaiian buoy 51004 from the global NWW3 model for December 2000. The old model (dashed line) shows a clear overestimation of observed wave heights (+). In the new model (solid line), this overestimation is mostly removed, indicating that the positive bias of the new model indeed could be attributed to the fact that the Hawaiian islands are not resolved in the NWW3 grid.

The effects of the continuous treatment of ice are less pronounced. In the global NWW3 model the effects are alternately positive and negative. In the regional AKW model, the effects are more systematically positive. In the WNA model, the effects of ice in general are negligible. For a more detailed discussion of the effects of the continuous treatment of ice, reference is made to section 5 Tolman (2002a).

5 RETUNING

Model changes have a tendency to 'de-tune' a model, even if the changes are based on proper physical or numerical considerations. This becomes particularly obvious if the original tuning of WAVEWATCH III is considered (Tolman, 2002e). This tuning was mostly performed by minimizing global wave model biases against altimeter data, using figures similar to Fig. 7. For the original model, bull's eye bias patterns due to unresolved islands as in this figure imply that such a tuning, at best, can be subjective. The new model

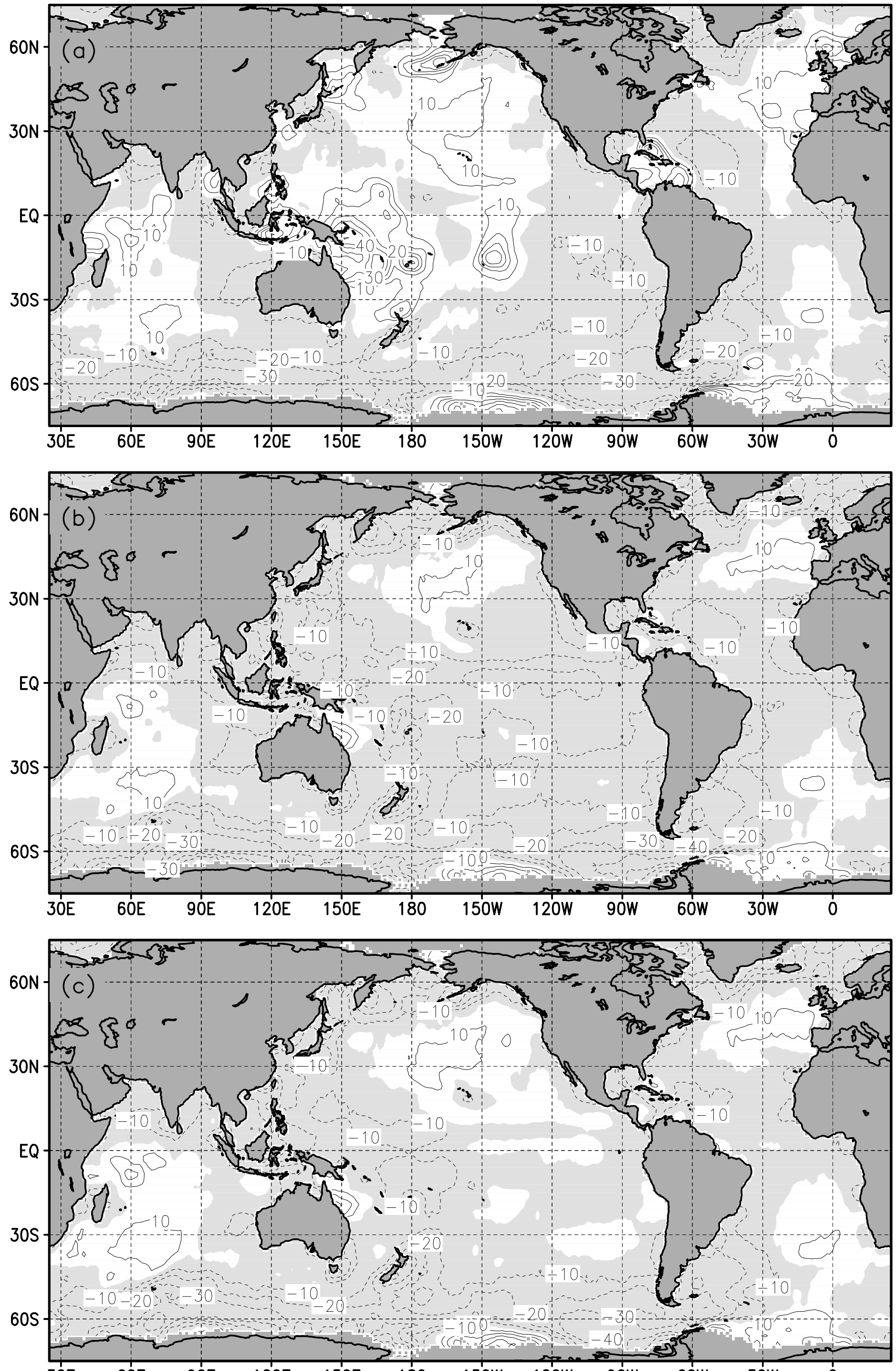

Fig. 7: Wave height biases in cm of the NWW3 model against ERS-2 altimeter data for March 2000 through February 2001. (a) Old model. (b) New model before retuning. (c) New model after retuning. Negative biases shaded light grey, contours at 10 cm intervals.

tuned as the old model (Fig. 7b) points to potential shortcomings in the original tuning, as it shows clear systematic bias patterns. The negative bias patterns in the tropics suggest that swell is attenuated too much by the winds. Similar conclusions have been drawn before by e.g., Wingeart et al. (2001). It is therefore prudent to revisit the original tuning of WAVEWATCH III.

This tuning focussed on the swell attenuation by wind, and on a general retuning of wave growth by means of an effective wind speed. The swell attenuation is a part of the input source term,

$$S_{i,m} = \begin{cases} S_i & \text{for} \quad \beta \geq 0 \quad \text{or} \quad f > 0.8 f_p \\ X_s S_i & \text{for} \quad \beta < 0 \quad \text{and} \quad f < 0.6 f_p \\ \mathcal{X}_s S_i & \text{for} \quad \beta < 0 \quad \text{and} \quad 06 f_p < f < 0.8 f_p \end{cases} , \tag{8}$$

where S_i is the original input source term, $S_{i,m}$ is the filtered source term, $\beta = S_i/(2\pi N)$ is the wind-wave interaction coefficient, f_p is the wind sea peak frequency (see Tolman, 1999, for details), X_s is the tunable filter factor, and $\mathcal{X}_s$ represents a linear reduction of X_s with f providing a smooth transition between the original and reduced input. The original tuning of the model resulted in $X_s = 0.125$. The effective wind speed U_e is used in the source terms instead of the actual wind speed U_{10},

$$U_e = \sqrt{c_o} U_{10} \quad . \tag{9}$$

Note that the actual effective wind speed also has a stability component, but that is irrelevant here. The original tuning of the model resulted in $c_o = 1.4$.

As is discussed in more detail in section 6 of Tolman (2002b), attempts at removing the systematic bias pattern of Fig. 7b have had only limited success. Changes in X_s and c_o to remove negative tropical biases in general increase positive biases at higher latitudes and vise versa. This indicates that the remaining bias pattern is a direct consequence of the limitations of the present parameterizations of the physics. In the new model the parameters are slightly modified to $X_s = 0.10$ and $c_o = 1.38$. The corresponding global bias patterns are shown in Fig. 7c.

6 OUTLOOK

After the recent new release of WAVEWATCH III, efforts to further improve the model performance will continue. Particularly with the inclusion of the sub-grid representation of islands, it is clear that the present default physics parameterizations leave room for improvement (see previous section). A major limitation in further development of source term parameterizations is the lack of an accurate and economical parameterizations of the nonlinear interactions. Presently, all third generation wave models use the Discrete Interaction Approximation (DIA) of Hasselmann et al. (1985). Although the DIA can be credited with making third-generation wave models feasible, its inherent limitations have become more and more clear in the last few years. This has lead to a concerted effort by the Office of Naval Research (ONR) to develop new parameterizations for the nonlinear interactions (e.g., Van Vledder et al., 2000). In this context, NCEP is working on Neural Network parameterizations of the nonlinear interactions (e.g., Krasnopolsky et al., 2002). It is expected that one or more alternative parameterizations of the nonlinear interactions will be available in the next release of WAVEWATCH III. As soon as such parameterizations become available, the input and dissipation source terms will be revisited as well.

Recently, coupled wind wave and atmosphere modeling for hurricanes has been in the center of interest. For such modeling, a wave model is required with multiple, moving nests, where the information from the high resolution grids is fed back to the lower resolution grids. Presently, WAVEWATCH III only feeds information from the lower resolution to the higher resolution. This in essence requires the development of a multi-scale wave model. In such a model, the large WNA and ENP domains can be replaced by much smaller high-resolution shelf areas, combined with dynamically adjusted hurricane nests. This has several advantages. (i) General model economy; high resolution is only used where needed. (ii) Hurricane swells will travel unimpeded across the globe, and not only within the specialized hurricane wave model. (iii) In such a model, it should be straightforward to incorporate ad-hoc high resolution wave grids, particularly for emergency response. The building of a general purpose multi-scale wave model will require a significant investment in development resources, and is expected to take place over the next four to five years.

References

Booij, N. and L. H. Holthuijsen, 1987: Propagation of ocean waves in discrete spectral wave models. *J. Comput. Physics*, **68**, 307–326.

Chao, Y. Y. and H. L. Tolman, 2001: Specification of hurricane wind fields for ocean wave prediction. in B. L. Edge and J. M. Hemsley, editors, *Ocean Wave Measurement and Analysis*, pp. 671–679. ASCE.

Hargreaves, J. C. and J. D. Annan, 1998: Integration of source terms in WAM. in *Proceedings of the 5th International Workshop on Wave Forecasting and Hindcasting*, pp. 128–133.

Hargreaves, J. C. and J. D. Annan, 2001: Comments on improvement of the short fetch behavior in the WAM model. *J. Atmos. Oceanic Techn.*, **18**, 711–715.

Hasselmann, K., T. P. Barnett, E. Bouws, H. Carlson, D. E. Cartwright, K. Enke, J. A. Ewing, H. Gienapp, D. E. Hasselmann, P. Kruseman, A. Meerburg, P. Mueller, D. J. Olbers, K. Richter, W. Sell and H. Walden, 1973: Measurements of wind-wave growth and swell decay during the Joint North Sea Wave Project (JONSWAP). *Ergaenzungsheft zur Deutschen Hydrographischen Zeitschrift, Reihe A(8)*, **12**, 95 pp.

Hasselmann, S., K. Hasselmann, J. H. Allender and T. P. Barnett, 1985: Computations and parameterizations of the nonlinear energy transfer in a gravity-wave spectrum, Part II: parameterizations of the nonlinear energy transfer for application in wave models. *J. Phys. Oceanogr.*, **15**, 1378–1391.

Holthuijsen, L. H., N. Booij, R. C. Ris, I. G. Haagsma, A. T. M. M. Kieftenburg and E. E. Kriezi, 2001: *SWAN Cycle III version 40.11 user manual*. Delft University of Technology, Department of Civil Engineering, P.O. Box 5048, 2600 GA Delft, The Netherlands, see http://swan.ct.tudelft.nl.

Krasnopolsky, V. M., D. V. Chalikov and H. L. Tolman, 2002: A neural network technique to improve computational efficiency of numerical oceanic models. *Ocean Mod.*, **4**, 363–383.

Leonard, B. P., 1979: A stable and accurate convective modelling procedure based on quadratic upstream interpolation. *Comput. Methods Appl. Mech. Engng.*, **18**, 59–98.

Leonard, B. P., 1991: The ULTIMATE conservative difference scheme applied to unsteady one-dimensional advection. *Comput. Methods Appl. Mech. Engng.*, **88**, 17–74.

Resio, D. T. and W. Perrie, 1991: A numerical study of nonlinear energy fluxes due to wave-wave interactions. Part 1: Methodology and basic results. *J. Fluid Mech.*, **223**, 609–629.

Tolman, H. L., 1992: Effects of numerics on the physics in a third-generation wind-wave model. *J. Phys. Oceanogr.*, **22**, 1095–1111.

Tolman, H. L., 1999: User manual and system documentation of WAVEWATCH III version 1.18. Tech. Note 166, NOAA/NWS/NCEP/OMB, 110 pp.

Tolman, H. L., 2001: Improving propagation in ocean wave models. in B. L. Edge and J. M. Hemsley, editors, *Ocean Wave Measurement and Analysis*, pp. 507–516. ASCE.

Tolman, H. L., 2002a: Alleviating the garden sprinkler effect in wind wave models. *Ocean Mod.*, **4**, 269–289.

Tolman, H. L., 2002b: Testing of WAVEWATCH III version 2.22 in NCEP's NWW3 ocean wave model suite. Tech. Note 214, NOAA/NWS/NCEP/OMB, 99 pp.

Tolman, H. L., 2002c: Treatment of unresolved islands and ice in wind wave models. *Ocean Mod.*, Accepted.

Tolman, H. L., 2002d: User manual and system documentation of WAVEWATCH III version 2.22. Tech. Note 222, NOAA/NWS/NCEP/OMB, 133 pp. (DRAFT).

Tolman, H. L., 2002e: Validation of WAVEWATCH III version 1.15 for a global domain. Tech. Note 213, NOAA/NWS/NCEP/OMB, 33 pp.

Tolman, H. L., B. Balasubramaniyan, L. D. Burroughs, D. V. Chalikov, Y. Y. Chao, H. S. Chen and V. M. Gerald, 2002: Development and implementation of wind generated ocean surface wave models at NCEP. *Wea. Forecasting*, **17**, 311–333.

Tolman, H. L. and D. V. Chalikov, 1996: Source terms in a third-generation wind-wave model. *J. Phys. Oceanogr.*, **26**, 2497–2518.

Tracy, B. and D. T. Resio, 1982: Theory and calculation of the nonlinear energy transfer between sea waves in deep water. WES Report 11, US Army Corps of Engineers.

Van Vledder, G. P., 2002: A subroutine version of the Webb/Resio/Tracy method for the computation of nonlinear quadruplet interactions in a wind-wave spectrum. Report 151a, Alkyon, The Netherlands.

Van Vledder, G. P., T. H. C. Herbers, R. E. Jenssen, D. T. Resio and B. Tracy, 2000: Modelling of non-linear quadruplet wave-wave interactions in operational wave models. in *Proc. 27nd Int. Conf. Coastal Eng., Sydney, Australia*, pp. 797–811. ASCE.

WAMDIG, 1988: The WAM model – a third generation ocean wave prediction model. *J. Phys. Oceanogr.*, **18**, 1775–1809.

Webb, D. J., 1978: Non-linear transfers between sea waves. *Deep-Sea Res.*, **25**, 279–298.

Wingeart, K. M., W. C. O'Reilly, T. H. C. Herbers, P. A. Wittmann, R. E. Jenssen and H. L. Tolman, 2001: Validation of operational global wave prediction models with spectral buoy data. in B. L. Edge and J. M. Hemsley, editors, *Ocean Wave Measurement and Analysis*, pp. 590–599. ASCE.